Kernel-based Image Reconstruction from scattered Radon data by (anisotropic) positive definite functions

Stefano De Marchi [1]

February 5, 2016

DIPARTIMENTO MATEMATICA

[1] Joint work with A. Iske (Hamburg, D), A. Sironi (Lousanne, CH) and G. Santin (Stuttgart, D)

Main references

1. S. De Marchi, A. Iske and A. Sironi, *Kernel-based Image Reconstruction from Scattered Radon Data by Positive Definite Functions*, submitted 2013 (download at http://www.math.unipd.it/~demarchi/papers/Kernel_based_image_reconstruction.pdf)
2. S. De Marchi, A. Iske and G. Santin, *Kernel-based Image Reconstruction from scattered Radon data by anisotropic positive definite functions*, Draft 2016
3. T. G. Feeman, The mathematics of medical imaging: a beginners guide , Springer 2010.
4. A. Iske, *Reconstruction of functions from generalized Hermite-Birkhoff data*. In: Approximation Theory VIII, Vol. 1: Approximation and Interpolation, C.K. Chui and L.L. Schumaker (eds.), World Scientific, Singapore, 1995, 257–264.
5. F. Natterer: The Mathematics of Computerized Tomography. Classics in Applied Mathematics, vol. 32. SIAM, Philadelphia, 2001
6. Amos Sironi, *Medical image reconstruction using kernel-based methods*, Master's thesis, University of Padua, 2011, arXiv:1111.5844v1.
7. Davide Poggiali, *Reconstruction of medical images from Radon data in trasmission and emission tomography*, Master's thesis, University of Padua, 2012.
8. Maria Angela Narduzzo, *A kernel method for CT reconstruction: a fast implementation using circulant matrices*, Master's thesis, University of Padua, Dec. 2013.
9. Silvia Guglielmo, *Stable kernel based methods for medical image reconstruction*, Master's thesis, University of Padua, Dec. 2013.

Part I

The problem and the first approach

Work with A. Iske, A. Sironi

Outline

Description of CT

How does it work?

- Non-invasive medical procedure (X-ray equipment).
- X-ray beam is assumed to be:
  - monochromatic;
  - zero-wide;
  - not subject to diffraction or refraction.
- Produce cross-sectional images.
- Transmission tomography (emissive tomography, like PET and SPECT, are not considererd here)

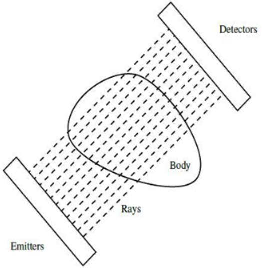

Description of CT

How does it work?

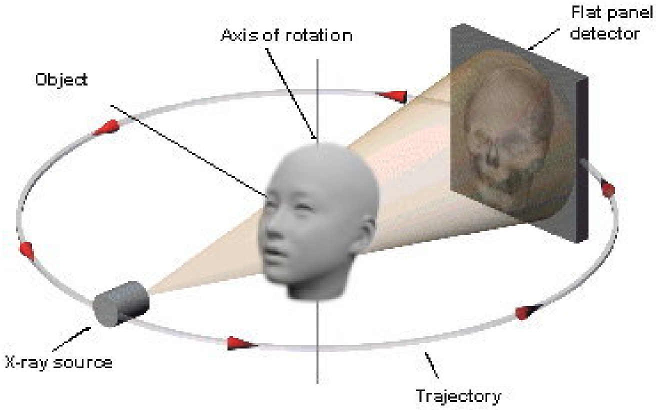

- $\ell_{(t,\theta)}$ $\longrightarrow$ line along which the X-ray is moving;
- $(t, \theta) \in \mathbb{R} \times [0, \pi)$ $\longrightarrow$ polar coordinates of line-points;
- f $\longrightarrow$ attenuation coefficient of the body;
- I $\longrightarrow$ intensity of the X-ray.

X-rays

- Discovered by Wihelm Conrad Röntgen in 1895
- Wavelength in the range $[0.01, 10] \times 10^{-9}$ m
- Attenuation coefficient:

$$A(x) \approx \text{"}\#\textit{pho.s absorbed}/1\ \textit{mm}\text{"}$$
$$A : \Omega \to [0, \infty)$$

Figure: First X-ray image: Frau Röntgen left hand.

CT machine and people

Computerized Tomography (CT)

modern CT

Allan Mcleod Cormack

Godfrey Newbold Hounsfield

both got Nobel Price for Medicine and Physiology in 1979

Computerized Axial Tomography

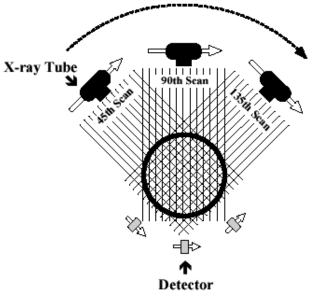

Figure: First generation of CT scanner design.

- A. Cormack and G. Hounsfield 1970
- Reconstruction from X-ray images taken from 160 or more beams at each of 180 directions
- Beer's law (loss of intensity):

$$\int_{x_0}^{x_1} A(x)\,dx = \underbrace{\ln\left(\frac{I_0}{I_1}\right)}_{\text{given by CT}}$$

Outline

Lines in the plane

A line l in the plane, perpendicular to the unit vector $\mathbf{n}_\theta = (\cos\theta, \sin\theta)$ and passing through the point $\mathbf{p} = (t\cos\theta, t\sin\theta) = t\mathbf{n}_\theta$, can be characterized (by the polar coordinates $t \in \mathbb{R}$, $\theta \in [0, \pi)$), i.e. $l = l_{t,\theta}$

$$l_{t,\theta} = \{\mathbf{x} := (t\cos\theta - s\sin\theta, t\sin\theta + s\cos\theta) = (x_1(s), x_2(s)) \;\; s \in \mathbb{R}\}$$

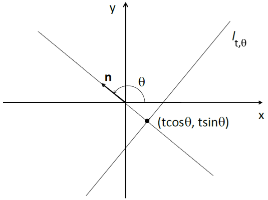

Figure: A line in the plane.

Radon transform

definition

The Radon transform of a given function $f : \Omega \subset \mathbb{R}^2 \to \mathbb{R}$ is defined for each pair of real number (t, θ), as line integral

$$Rf(t,\theta) = \int_{l_{t,\theta}} f(\mathbf{x})d\mathbf{x} = \int_{\mathbb{R}} f(x_1(s), x_2(s))\, ds$$

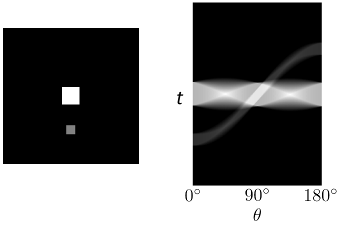

Figure: Left: image. Right: its Radon transform (*sinogram*)

Radon tranform

Image reconstruction

A CT scan measures the X-ray projections through the object, producing a sinogram, which is effectively the Radon transform of the attenuation coefficient function f in the (t, θ)-plane.

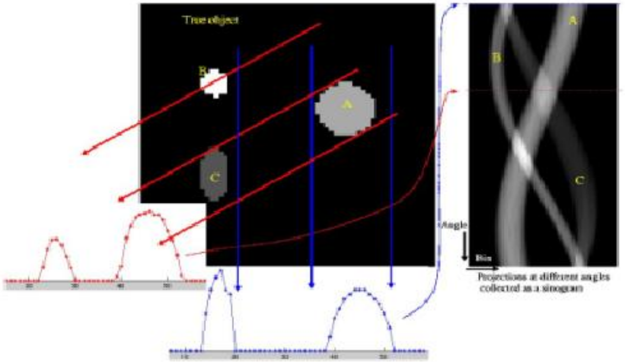

Radon transform: another example

Figure: Shepp-Logan phantom.

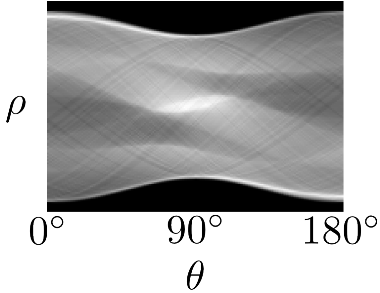

Figure: Radon transform (*sinogram*).

Back projection

- First attempt to recover f from Rf
- The back projection of the function $h \equiv h(t, \theta)$ is the transform

$$Bh(\mathbf{x}) = \frac{1}{\pi} \int_0^{\pi} h(x_1 \cos\theta + x_2 \sin\theta, \theta)\, d\theta$$

i.e. the average of h over the angular variable θ, where $t = x_1 \cos\theta + x_2 \sin\theta = \mathbf{x}^T \mathbf{n}_\theta$.

Figure: Back projection of the Radon transform.

Important theorems

Theorem (*Central Slice Theorem*)

For any suitable function f defined on the plane and all real numbers r, θ

$$F_2 f(r\cos\theta, r\sin\theta) = F(Rf)(r,\theta).$$

(F_2 and F are the 2-d and 1-d Fourier transforms, resp.).

Theorem (*The Filtered Back-Projection Formula*)

For a suitable function f defined in the plane

$$f(\mathbf{x}) = \frac{1}{2} B\{F^{-1}[|r| F\,(Rf)(r,\theta))]\}(\mathbf{x})\,, \quad \mathbf{x} \in \mathbb{R}^2.$$

Fundamental question

Fundamental question of image reconstruction.

Is it possible to reconstruct a function f starting from its Radon transform Rf? □

Answer (Radon 1917).

Yes, we can if we know the value of the Radon transform for all r, θ. □

Discrete problem

DIPARTIMENTO MATEMATICA

Ideal case

- $Rf(t, \theta)$ known for all t, θ
- Infinite precision
- No noise

Real case

- $Rf(t, \theta)$ known only on a finite set $\{(t_j, \theta_k)\}_{j,k}$
- Finite precision
- Noise in the data

Fourier-based approach

- Sampling: $Rf(t,\theta) \to R_D f(jd, k\pi/N)$
- Discrete transform: e.g.

$$B_D h(\mathbf{x}) = \frac{1}{N}\sum_{k=0}^{N-1} h(x\cos(k\pi/N) + y\sin(k\pi/N), k\pi/N)$$

- Filtering (low-pass): $|r| = F\phi(r)$, with ϕ band-limited function
- Interpolation: $\{f_k \; : \; k \in \mathbb{N}\} \; \to \; If(x), \; x \in \mathbb{R}$

Discrete problem

- Filtered Back-Projection Formula

$$f(\mathbf{x}) = \frac{1}{2} B\{F^{-1}[|r| \cdot F(Rf(r,\theta))]\}(\mathbf{x})$$

- Filtering

$$\begin{aligned} f(\mathbf{x}) &= \frac{1}{2} B\{F^{-1}[F(\phi(r)) \cdot F(Rf(r,\theta))]\}(\mathbf{x}) = \\ &= \frac{1}{2} B\{F^{-1}[F(\phi * Rf(r,\theta))]\}(\mathbf{x}) \\ &= \frac{1}{2} B[\phi * Rf(r,\theta)](\mathbf{x}) \end{aligned}$$

- Sampling and interpolation

$$f(x_1^m, x_2^n) = \frac{1}{2} B_D I[\phi * R_D f(r_j, \theta_k)](x_1^m, x_2^n)$$

Discrete problem: an example

Figure: Shepp-Logan phantom.

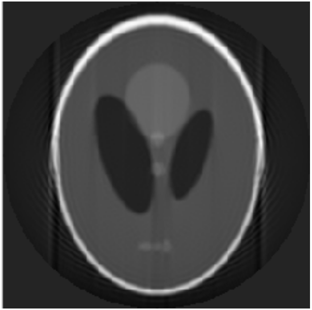

Figure: Reconstruction with linear interpolation and $180x101 = 18180$ samples.

Outline

1. Image Reconstruction from CT
2. Radon transform
3. Alg. Rec. Tech. (ART), Kernel approach
   - Regularization
   - Numerical results

Algebraic Reconstruction Techniques (ART)

Differently from Fourier-based reconstruction, we consider $\mathcal{G} = \mathrm{span}\{g_j,\ j = 1, ..., n\}$ of n basis functions and we solve the reconstruction problem on all Radom lines $\mathcal{L}$

$$R_{\mathcal{L}}(g) = R_{\mathcal{L}}(f)$$

by using

$$g = \sum_{j=1}^{n} c_j g_j \,.$$

- Asking interpolation, that is

  $$Rg(t_k, \theta_k) = Rf(t_k, \theta_k), \quad k = 1, \ldots, m$$

  we obtain the linear system $A\mathbf{c} = \mathbf{b}$ with
  $A_{k,j} = Rg_j(t_k, \theta_k), \quad k = 1, \ldots, m,\ j = 1, \ldots, n\,.$
- Large, often sparse, linear system
- Solution by iterative methods (Kaczmarz, MLEM, OSEM, LSCG), or SIRT techniques (see **AIRtools** by Hansen &Hansen 2012).

ART reconstruction: Example 1

Figure: Bull's eye phantom.

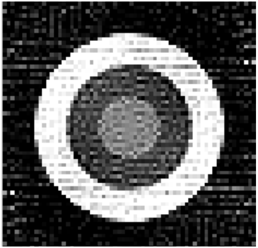

Figure: $64 \times 64 = 4096$ reconstructed image with 4050 samples by Kaczmarz.

ART reconstruction: Example 2

Figure: Shepp-Logan phantom.

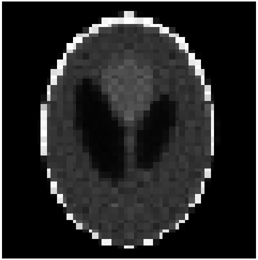

Figure: The phantom reconstructed by MLEM in 50 iterations.

Hermite-Birkhoff interpolation

Let $\Lambda = \{\lambda_1, \ldots, \lambda_n\}$ be a set of linearly independent linear functionals and $f_\Lambda = (\lambda_1(f), \ldots, \lambda_n(f))^T \in \mathbb{R}^n$.
The solution of a general H-B reconstruction problem:

H-B reconstruction problem

find g such that $g_\Lambda = f_\Lambda$ or

$$\lambda_k(g) = \lambda_k(f), \quad k = 1, \ldots, n.$$

Hermite-Birkhoff interpolation

DIPARTIMENTO MATEMATICA

Let $\Lambda = \{\lambda_1, \ldots, \lambda_n\}$ be a set of linearly independent linear functionals and $f_\Lambda = (\lambda_1(f), \ldots, \lambda_n(f))^T \in \mathbb{R}^n$.
The solution of a general H-B reconstruction problem:

H-B reconstruction problem

find g such that $g_\Lambda = f_\Lambda$ or

$$\lambda_k(g) = \lambda_k(f), \quad k = 1, \ldots, n\,.$$

- In our setting the functionals are

$$\lambda_k := R_k f = Rf(t_k, \theta_k), \quad k = 1, \ldots, n$$

- The interpolation conditions

$$\sum_{j=1}^{n} c_j \lambda_k(g_j) = \lambda_k(f), \quad k = 1, \ldots, n$$

that corresponds to the linear system $A\mathbf{c} = \mathbf{b}$ as before.

Hermite-Birkhoff interpolation

DIPARTIMENTO MATEMATICA

Theorem (Haar-Mairhuber-Curtis)

If $\Omega \subset \mathbb{R}^d$, $d \geq 2$ contains an interior point, there exist no Haar spaces of continuous functions except the 1-dimensional case.

- The well-posedness of the interpolation problem is garanteed if we no longer fix in advance the set of basis functions.
- Thus, the basis g_j should depend on the data:

$$g_j(\mathbf{x}) = \lambda_j^y(K(\mathbf{x},\mathbf{y})) \;\; [= R^{\mathbf{y}}[K(\mathbf{x},\mathbf{y})](t_k,\theta_k)] \,, \quad j = 1,\ldots,n$$

with the kernel K such that the matrix

$$A = (\lambda_j^{\mathbf{x}}[\lambda_k^{\mathbf{y}}(K(\mathbf{x},\mathbf{y}))])_{j,k}$$

is not singular $\forall \; (t_j,\theta_j)$

Positive definite radial kernels

DIPARTIMENTO MATEMATICA

We choose a kernel $K : \mathbb{R}^2 \times \mathbb{R}^2 \to \mathbb{R}$ continuous

- Symmetric $K(\mathbf{x}, \mathbf{y}) = K(\mathbf{y}, \mathbf{x})$
- Radial $K(\mathbf{x}, \mathbf{y}) = \Phi_\epsilon(\|\mathbf{x} - \mathbf{y}\|), \ \epsilon > 0$
- Positive definite (PD)

$$\sum_{k,j=1}^{n} c_j c_k \lambda_j^{\mathbf{x}} \lambda_k^{\mathbf{y}} K(\mathbf{x}, \mathbf{y}) \geq 0$$

for all set of linear operators λ_j and for all $c \in \mathbb{R}^n \setminus \{0\}$

Positive definite kernels: examples

DIPARTIMENTO MATEMATICA

- Gaussian

$$\Phi_\epsilon(||\mathbf{x}||) = e^{-(\epsilon||\mathbf{x}||)^2}, \quad PD \ \forall \ \mathbf{x} \in \mathbb{R}^2, \epsilon > 0$$

- Inverse multiquadrics

$$\Phi_\epsilon(||\mathbf{x}||) = \frac{1}{\sqrt{1 + (\epsilon||\mathbf{x}||)^2}}, \quad PD \ \forall \ \mathbf{x} \in \mathbb{R}^2, \ \epsilon > 0$$

- Askey's compactly supported (or radial characteristic function)

$$\Phi_\epsilon(||\mathbf{x}||) = (1 - \epsilon||\mathbf{x}||)_+^\beta = \begin{cases} (1 - \epsilon||\mathbf{x}||)^\beta & ||\mathbf{x}|| < 1/\epsilon \\ 0 & ||\mathbf{x}|| \geq 1/\epsilon \end{cases}$$

which are PD for any $\beta > 3/2$.

A useful Lemma

Lemma

Let $K(\mathbf{x}, \mathbf{y}) = \phi(\|\mathbf{x} - \mathbf{y}\|)$ *with* $\phi \in L^1(\mathbb{R})$. *Then for any* $\mathbf{x} \in \mathbb{R}^2$ *the Radon transform* $R^{\mathbf{y}} K(\mathbf{x}, \mathbf{y})$ *at* $(t, \theta) \in \mathbb{R} \times [0, \pi)$ *can be expressed*

$$(R^{\mathbf{y}} K(\mathbf{x}, \mathbf{y}))(t, \theta) = (R^{\mathbf{y}} K(\mathbf{0}, \mathbf{y}))(t - \mathbf{x}^T \mathbf{n}_\theta, \theta)\,.$$

A useful Lemma

Lemma

Let $K(\mathbf{x},\mathbf{y}) = \phi(\|\mathbf{x}-\mathbf{y}\|)$ *with* $\phi \in L^1(\mathbb{R})$. *Then for any* $\mathbf{x} \in \mathbb{R}^2$ *the Radon transform* $R^{\mathbf{y}}K(\mathbf{x},\mathbf{y})$ *at* $(t,\theta) \in \mathbb{R} \times [0,\pi)$ *can be expressed*

$$(R^{\mathbf{y}}K(\mathbf{x},\mathbf{y}))(t,\theta) = (R^{\mathbf{y}}K(\mathbf{0},\mathbf{y}))(t-\mathbf{x}^T\mathbf{n}_\theta,\theta)\,.$$

This is the so-called shift invariant property of the Radon transform!

Problem

- Inverse multiquadric kernel

$$K(\mathbf{x}, \mathbf{y}) = \frac{1}{\sqrt{1 + \|\mathbf{x} - \mathbf{y}\|^2}}.$$

Applying the previous Lemma we have

$$R^{\mathbf{y}}[K(\mathbf{0}, \mathbf{y})](t, \theta) = \int_{\mathbb{R}} \frac{1}{\sqrt{1 + t^2 + s^2}} \, ds = +\infty$$

$\longrightarrow$ the basis g_j and the matrix A are not well defined $\longleftarrow$

Regularization

Window function

- Multiplying the kernel K for a "window function" w such that

$$R[K(\mathbf{x}, \mathbf{y})w](t, \theta) < \infty \quad \forall\ (\mathbf{x}, \mathbf{y}), (t, \theta).$$

- This corresponds to use the linear operator R_w in place of R

$$R_w[f](t, \theta) = R[fw](t, \theta).$$

- We consider w radial: $w = w(\|\cdot\|)$

Example of window functions

- Characteristic function

$$w(\mathbf{x}) = \chi_{[-L,L]}(\|\mathbf{x}\|),\ L > 0$$

- Gaussian

$$w(\mathbf{x}) = e^{-\nu^2\|\mathbf{x}\|^2},\ \nu > 0$$

- Compactly supported (Askey's family)

$$w(\mathbf{x}) = (1 - \nu^2\|\mathbf{x}\|^2)_+,\ \nu > 0$$

Example: gaussian kernel

- Gaussian kernel, shape parameter ε

$$K(\mathbf{x},\mathbf{y}) = e^{-\varepsilon^2\|\mathbf{x}-\mathbf{y}\|^2}, \ \varepsilon > 0$$

- Basis function

$$g_j(\mathbf{x}) = R^{\mathbf{y}}[K(\mathbf{x},\mathbf{y})](t_j,\theta_j) = \frac{\sqrt{\pi}}{\varepsilon} e^{-\varepsilon^2(t_j-\mathbf{x}^T\mathbf{v}_j)^2}$$

with $\mathbf{v}_j = (\cos\theta_j, \sin\theta_j)$

- Matrix $A = (a_{k,j})$

$$a_{k,j} = R[g_j](t_k,\theta_k) = +\infty, \quad \text{if } \theta_j = \theta_k$$

Example: gaussian kernel

- Gaussian window function

$$w(\mathbf{x}) = e^{-\nu^2\|\mathbf{x}\|^2},\ \nu > 0$$

- Matrix A becomes

$$a_{k,j} = R[g_j\, w](t_k, \theta_k) = \frac{\pi \exp\left[-\nu^2\left(t_k^2 + \frac{\varepsilon^2 b^2}{\varepsilon^2 a^2 + \nu^2}\right)\right]}{\varepsilon \sqrt{\varepsilon^2 a^2 + \nu^2}}$$

where $a = \sin(\theta_k - \theta_j)$ and $b = t_j - t_k \cos(\theta_k - \theta_j)$
which is never vanishing!

Example: gaussian kernel reconstruction

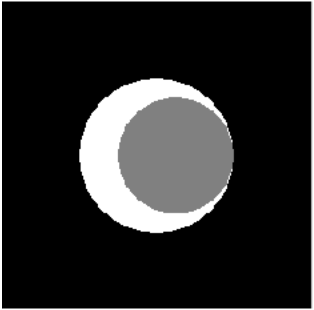

Figure: Crescent-shaped phantom.

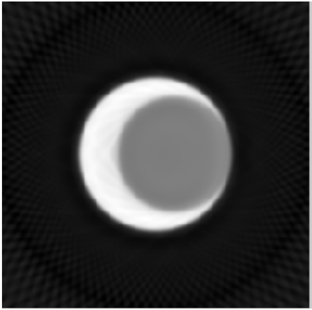

Figure: $256 \times 256 = 65536$ reconstructed image with $n = 4050$ samples.

A numerical experiment

- Gaussian kernel Φ_ϵ and gaussian weight w_ν
- Comparison with the Fourier-based reconstruction (relying on the FBP)
- Reconstructions from scattered Radon data and noisy Radon data
- Root Mean Square Error

$$RMSE = \frac{1}{J}\sqrt{\sum_{i=1}^{J}(f_i - g_i)^2}$$

J is the dimension of the image, $\{f_i\}, \{g_i\}$ the greyscale values at the pixels of the original and the reconstructed image.

Kernel-based vs Fourier based: I

◇ Test phantoms

Figure: crescent shape

Figure: bull's eye

Figure: Shepp-Logan

Geometries

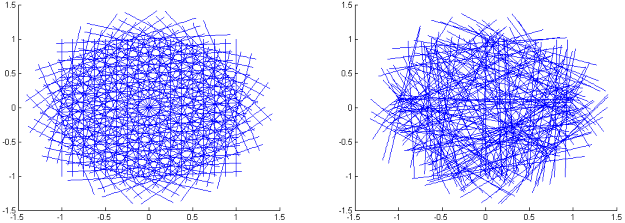

Figure: Left: parallel beam geometry, 170 lines (10 angles and 17 Radon lines per angle). Right: scattered Radon lines, 170 lines.

Kernel-based vs Fourier based: II

- Using parallel beam geometry, i.e. $\theta_k = k\pi/N, \; k = 0, \ldots, N-1$ and $t_j = jd, \; j = -M, \ldots, M$, with sampling spacing $d \longrightarrow 0$, $(2M+1) \times N$ regular grid of Radon lines.

  No noise on the data.

- With $N = 45, \; M = 40, \; \epsilon = 60$ we got

Phantom	optimal ν	kernel-based	Fourier-based
crescent	0.5	0.102	0.120
bull's eye	0.4	0.142	0.134

Table: RMSE of kernel-based vs Fourier-based method

Kernel-based vs Fourier based: III

DIPARTIMENTO MATEMATICA

- Using scattered Radon data, with increasing randomly chosen Radon lines $n = 2000, 5000, 10000, 20000$.

  No noise on the data.

- With $\epsilon = 50$ and $\nu = 0.7$

Phantom	2000	5000	10000	20000
crescent	0.1516	0.1405	0.1431	0.1174
bull's eye	0.1876	0.1721	0.2102	0.1893

Table: RMSE of kernel-based vs different number n of Radon lines

Kernel-based vs Fourier based: IV

These experiments are with noisy Radon data, i.e. we add a gaussian noise of zero mean and variance $\sigma = 1.e - 3$ to each of the three phantoms.

- Parallel beam geometry, same ϵ and ν

Phantom	kernel-based	Fourier-based
crescent	0.1502	0.1933
bull's eye	0.1796	0.2322

Table: RMSE of kernel-based vs Fourier-based with noisy data

- Scattered Radon data, same ϵ and ν

Phantom	noisy	noisy-free
crescent	0.2876	0.1820
bull's eye	0.3140	0.2453

Table: RMSE with noisy and noisy-free data

Window function parameter

- Gaussian kernel; Gaussian window function

$$K(\mathbf{x},\mathbf{y}) = e^{-\varepsilon^2\|\mathbf{x}-\mathbf{y}\|^2} \qquad w(\mathbf{x}) = e^{-\nu^2\|\mathbf{x}\|^2}$$

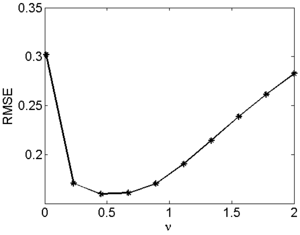

(a) *RMSE* (b) $k^{-1}(A)$

Figure: Bull's eye phantom, $\varepsilon = 30$.

- Trade-off principle (Schaback 1995)

Kernel shape parameter

- Multiquadric kernel, Gaussian window

$$K(\mathbf{x}, \mathbf{y}) = \sqrt{1 + \rho^2 \|\mathbf{x} - \mathbf{y}\|^2}\, e^{-\varepsilon^2 \|\mathbf{x} - \mathbf{y}\|^2}$$

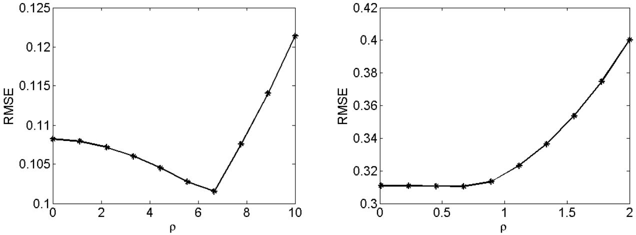

(a) Crescent-shaped phantom (b) Shepp-Logan phantom

Figure: Optimal values depend on the data.

- Optimal values depend on data.

Comparison with FBP Formula

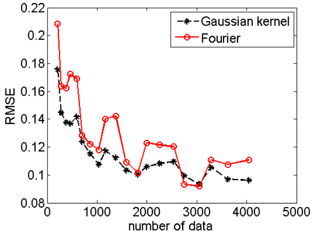

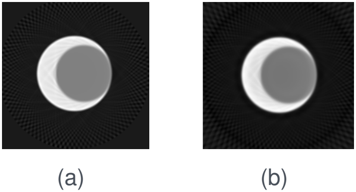

Figure: FBP and Gaussian kernel reconstruction (with optimal parameters ε^*, ν^*).

Figure: Crescent-shaped: (a) FBP; (b) Gaussian kernel.

Comparison with FBP Formula

* *RMSE* of the same order (ok!)
* More computational time and memory usage (not so well!)

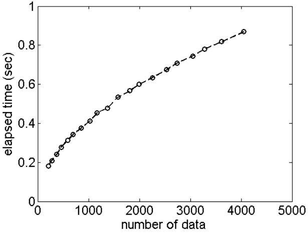

(a) FBP

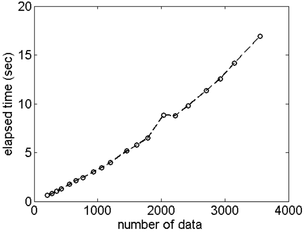

(b) Multiquadric kernel

Figure: Computational time.

Part II

Double weighted kernel-method

Work with A. Iske and G. Santin

Outline

Isotropic and anisotropic kernels

- Isotropic (radially symmetric) kernel

$$K(\mathbf{x}, \mathbf{y}) = \varphi(\|\mathbf{x} - \mathbf{y}\|^2), \quad (\mathbf{x}, \mathbf{y}) \in \mathbb{R}^2$$

- Anisotropic (symmetric) kernel

$$K(\mathbf{x}, \mathbf{y}) = \varphi(\|\mathbf{x} - \mathbf{y}\|^2) w(\|\mathbf{x}\|^2) w(\|\mathbf{y}\|^2), \quad (\mathbf{x}, \mathbf{y}) \in \mathbb{R}^2 \tag{1}$$

where $w : [0, \infty) \to [0, \infty)$ suitable weight function

Well definitness of the basis functions g_j

Consider the *Schwartz space* (cf. Iske 94)

$$\mathcal{S} := \{\gamma \in C^{\infty}(\mathbb{R}^d;\mathbb{R}) : D^p\gamma(\mathbf{x})\mathbf{x}^q \to 0, \quad \forall\, p,q \in \mathbb{N}_0^d\}$$

i.e. the set of rapidly decaying C^{∞} functions.

Definition

A continuous and symmetric function $K : \mathbb{R}^d \times \mathbb{R}^d \longrightarrow \mathbb{R}$ is said to be positive definite on $\mathcal{S}$, $K \in PD(\mathcal{S})$ iff

$$\int_{\mathbb{R}^d}\int_{\mathbb{R}^d} K(\mathbf{x},\mathbf{y})\gamma(\mathbf{x})\gamma(\mathbf{y})d\mathbf{x}d\mathbf{y} > 0$$

for all $\gamma \in \mathcal{S} \setminus \{0\}$.

Construction of the anisotropic basis: I

- For the weighted kernels with K anisotropic, the basis functions are

$$g_{t,\theta}(\mathbf{x}) = R^{\mathbf{y}}_{t,\theta}\left[\varphi(\|\mathbf{x}-\mathbf{y}\|^2)w(\|\mathbf{y}\|^2)\right]w(\|\mathbf{x}\|^2) \quad (t,\theta)\in\mathbb{R}\times[0,\pi)$$

where $R_{t,\theta}$ is the Radon transform on the line $\ell = \ell_{t,\theta}$.

- Simplyfing notation

$$g(\mathbf{x}) = h_{t,\theta}(\mathbf{x})w(\mathbf{x})$$

where

$$h_{t,\theta}(\mathbf{x}) = R^{\mathbf{y}}_{t,\theta}\left[\varphi(\|\mathbf{x}-\mathbf{y}\|^2)w(\|\mathbf{y}\|^2)\right] = \int_{\ell_{t,\theta}}\varphi(\|\mathbf{x}-\mathbf{y}\|^2)w(\|\mathbf{y}\|^2)d\mathbf{y}$$

Construction of the anisotropic basis: II

Introducing the rotation matrix

$$Q_\theta = \begin{bmatrix} \cos(\theta) & -\sin(\theta) \\ \sin(\theta) & \cos(\theta) \end{bmatrix} = [\mathbf{n}_\theta, \mathbf{n}_\theta^\perp]$$

and letting $\mathbf{x}_\theta = Q_\theta^{-1}\mathbf{x} = Q_\theta^T\mathbf{x} = [\mathbf{x}^T\mathbf{n}_\theta, \mathbf{x}^T\mathbf{n}_\theta^\perp] \in \mathbb{R}^2$ we get

$$\begin{aligned} h_{t,\theta}(\mathbf{x}) &= \int_{\ell_{t,\theta}} \varphi(\|\mathbf{x}-\mathbf{y}\|^2) w(\|\mathbf{y}\|^2) d\mathbf{y} = \\ &= \int_{\ell_{t,0}} \varphi(\|\mathbf{x}-Q_\theta\mathbf{y}\|^2) w(\|Q_\theta\mathbf{y}\|^2) d\mathbf{y} \\ &= \int_{\ell_{t,0}} \varphi(\|Q_\theta^{-1}\mathbf{x}-\mathbf{y}\|^2) w(\|\mathbf{y}\|^2) d\mathbf{y} = \\ &= \int_{\ell_{t,0}} \varphi(\|\mathbf{x}_\theta-\mathbf{y}\|^2) w(\|\mathbf{y}\|^2) d\mathbf{y} \end{aligned}$$

Construction of the anisotropic basis: III

Any $\mathbf{y} \in \ell_{t,0}$ has the form $\mathbf{y} = [t, s]^T \in \mathbb{R}^2$ for a parameter $s \in \mathbb{R}$.
Setting $\mathbf{v}_{t,s} = [t, s]^T = \mathbf{y}$ we have

$$h_{t,\theta}(\mathbf{x}) = \int_{\mathbb{R}} \varphi((\mathbf{x}^T \mathbf{n}_\theta - t)^2 + (\mathbf{x}^T \mathbf{n}_\theta^\perp - s)^2) w(\|\mathbf{v}_{t,s}\|^2) ds$$

Construction of the anisotropic basis: III

Any $\mathbf{y} \in \ell_{t,0}$ has the form $\mathbf{y} = [t, s]^T \in \mathbb{R}^2$ for a parameter $s \in \mathbb{R}$.
Setting $\mathbf{v}_{t,s} = [t, s]^T = \mathbf{y}$ we have

$$h_{t,\theta}(\mathbf{x}) = \int_{\mathbb{R}} \varphi((\mathbf{x}^T\mathbf{n}_\theta - t)^2 + (\mathbf{x}^T\mathbf{n}_\theta^\perp - s)^2) w(\|\mathbf{v}_{t,s}\|^2) ds$$

Proposition

For any anisotropic kernel K of the our form, the basis functions $g_{t,\theta}$ have the form

$$g_{t,\theta}(\mathbf{x}) = \left[\int_{\mathbb{R}} \varphi((\mathbf{x}^T\mathbf{n}_\theta - t)^2 + (\mathbf{x}^T\mathbf{n}_\theta^\perp - s)^2) w(\|\mathbf{v}_{t,s}\|^2) ds\right] w(\|\mathbf{x}\|^2) \,. \quad (2)$$

Hence for $(\varphi\, w)(|\cdot|)^2 \in L^1(\mathbb{R})$ the functions $g_{t,\theta} : \mathbb{R}^2 \to [0, \infty)$ are well-defined.

Reconstruction matrix entries: I

DIPARTIMENTO MATEMATICA

The reconstruction problem $R_{\mathcal{L}}(g) = R_{\mathcal{L}}(f)$ amounts to solving a linear system $A\mathbf{c} = \mathbf{b}$ with matrix entries

$$a_{r,\phi}^{t,\theta} := R_{r,\phi}^{\mathbf{x}}[g_{t,\theta}(\mathbf{x})] = R_{t,\phi}^{\mathbf{x}}\left[R_{t,\theta}^{\mathbf{y}}\left[\varphi(\|\mathbf{x}-\mathbf{y}\|^2)w(\|\mathbf{y}\|^2)\right]w(\|\mathbf{x}\|^2)\right].$$

Reconstruction matrix entries: II

By using the representation of the basis functions $g_{t,\theta}$ (omitting the algebra) we get

Proposition

For $(t,\theta),(r,\phi) \in \mathbb{R} \times [0,\pi)$ we have

$$a_{r,\phi}^{t,\theta} = \int_{\mathbb{R}} \int_{\mathbb{R}} \varphi(\|Q_\phi \mathbf{v}_{r,\tilde{s}} - Q_\theta \mathbf{v}_{t,s}\|^2) w(\|\mathbf{v}_{t,s}\|^2) w(\|\mathbf{v}_{t,\tilde{s}}\|^2) ds\, d\tilde{s}$$

Again, if $(\varphi w)(|\cdot|^2) \in L^1(\mathbb{R})$ then the entries are well-defined and the reconstruction matrix

$$A = \left(a_{r_k,\phi_k}^{t_j,\theta_j}\right)_{1 \le j,k \le n} \in \mathbb{R}^{n \times n}$$

is symmetric positive definite.

In particular the diagonal entries are

$$a_{t,\theta}^{t,\theta} = \int_{\mathbb{R}} \int_{\mathbb{R}} \varphi((\tilde{s}-s)^2) w(s^2+t^2) w(\tilde{s}^2+t^2) ds\, d\tilde{s}\,.$$

Example: gaussian kernel

In the case of the Gaussian kernel $\varphi(\|\mathbf{x}-\mathbf{y}\|^2) = e^{-\varepsilon^2\|\mathbf{x}-\mathbf{y}\|^2}$ and weight $w(x) = exp(-\nu^2\|x\|^2)$ we get

$$g_{t,\theta}(\mathbf{x}) = \frac{\sqrt{\pi}}{\sqrt{\varepsilon^2+\nu^2}} \exp\left[-(\varepsilon^2+\nu^2)(t^2+\|\mathbf{x}\|^2) + 2\varepsilon^2 t\mathbf{n}_\theta\cdot\mathbf{x} + \frac{\varepsilon^4}{\varepsilon^2+\nu^2}(\mathbf{n}_\theta^\perp\cdot\mathbf{x})^2\right]$$

Matrix entries [DeMIS15]

For $(t,\theta),(r,\phi) \in \mathbb{R}\times[0,\pi)$ the entries of the gaussian kernel matrix are the Radon transform of the gaussian basis $g_{t,\theta}$ w.r.t. the line $\ell_{r,\phi}$, that is $a_{j,k} = R_{r,\phi}[g_{t,\theta}]$

$$\begin{aligned}
a_{j,k}\left(= a_{r,\phi}^{t,\theta}\right) &= \frac{\pi\sqrt{2}}{\sqrt{h_{\varepsilon,\nu}(\theta,\phi)}}\exp[\Phi_{\varepsilon,\nu}(r,t,\theta,\phi)] \\
\Phi_{\varepsilon,\nu}(r,t,\theta,\phi) &= -2\nu^2(2\varepsilon^2+\nu^2)\left(\frac{(\varepsilon^2+\nu^2)(r^2+t^2)-2\varepsilon^2 rt\cos(\theta-\phi)}{h_{\varepsilon,\nu}(\theta,\phi)}\right) \\
h_{\varepsilon,\nu}(\theta,\phi) &= 2(\varepsilon^2+\nu^2)^2 - 2\varepsilon^4\cos^2(\theta-\phi).
\end{aligned}$$

Example: gaussian kernel

In the case of the Gaussian kernel $\varphi(\|\mathbf{x}-\mathbf{y}\|^2) = e^{-\varepsilon^2\|\mathbf{x}-\mathbf{y}\|^2}$ and weight $w(x) = exp(-\nu^2\|x\|^2)$ we get

$$g_{t,\theta}(\mathbf{x}) = \frac{\sqrt{\pi}}{\sqrt{\varepsilon^2+\nu^2}} \exp\left[-(\varepsilon^2+\nu^2)(t^2+\|\mathbf{x}\|^2) + 2\varepsilon^2 t\mathbf{n}_\theta \cdot \mathbf{x} + \frac{\varepsilon^4}{\varepsilon^2+\nu^2}(\mathbf{n}_\theta^\perp \cdot \mathbf{x})^2\right]$$

Matrix entries [DeMIS15]

For $(t,\theta),(r,\phi) \in \mathbb{R} \times [0,\pi)$ the entries of the gaussian kernel matrix are the Radon transform of the gaussian basis $g_{t,\theta}$ w.r.t. the line $\ell_{r,\phi}$, that is $a_{j,k} = R_{r,\phi}[g_{t,\theta}]$

$$\begin{aligned}
a_{j,k}\left(= a_{r,\phi}^{t,\theta}\right) &= \frac{\pi\sqrt{2}}{\sqrt{h_{\varepsilon,\nu}(\theta,\phi)}} \exp[\Phi_{\varepsilon,\nu}(r,t,\theta,\phi)] \\
\Phi_{\varepsilon,\nu}(r,t,\theta,\phi) &= -2\nu^2(2\varepsilon^2+\nu^2)\left(\frac{(\varepsilon^2+\nu^2)(r^2+t^2) - 2\varepsilon^2 rt\cos(\theta-\phi)}{h_{\varepsilon,\nu}(\theta,\phi)}\right) \\
h_{\varepsilon,\nu}(\theta,\phi) &= 2(\varepsilon^2+\nu^2)^2 - 2\varepsilon^4\cos^2(\theta-\phi).
\end{aligned}$$

$\longrightarrow$ The matrix results symmetric and positive definite $\longleftarrow$

Example: bull-eye phantom

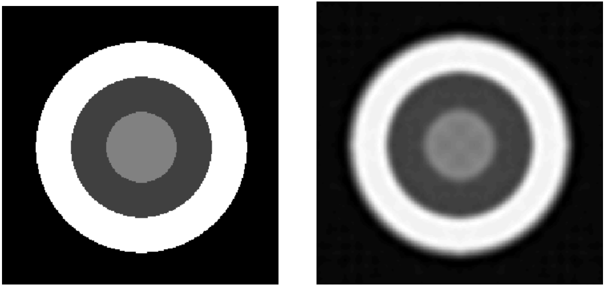

Figure: Bull-eye phantom, 64×64.
Left: original.
Right: Approximed with parallel beam, $\epsilon = 26$ and $\nu = 0.3333$.
RMSE=1.12e-1, PSNR=67.2

Example: Shepp-Logan phantom

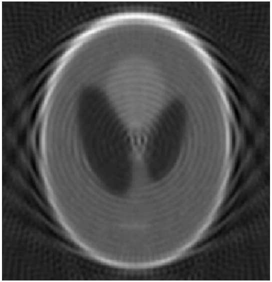

Figure: Shepp-Logan phantom, 64×64.
Left: original.
Right: Approximed with parallel beam, $\epsilon = 26$ and $\nu = 0.3333$.
RMSE=2.2e-1, PSNR=61.2

Outline

Newton Bases [MS JAT2011, PS JCAM2011]

Theorem (Basis factorization)

Any data-dependent basis U arises from a factorization $A = V_U \cdot C_U^{-1}$ where $V_U = (u_j(x_i))_{1\le i,j\le n}$ and $U(x) = (u_1(x), \cdots, u_n(x)) \in \mathbb{R}^n$ is a data-dependend basis; the coefficient matrix C_U is s.t.

$$U(x) = T(x) \cdot C_U$$

where $T(x) = (K(x, x_1), \cdots, K(x, x_n))$.

Observation

The matrix $A_{K_{ww},R}$ is symmetric and positive definite, $A = L \cdot L^t$ (Cholesky decomposition).

The Cholesky decomposition leads to the Newton basis, say $N(x)$

$$N(x) = T(x) \cdot C_N = T(x) \cdot (V_N)^{-t}\,. \tag{3}$$

Newton Bases

Observation

The Cholesky algorithm is recursive so we can construct the Newton Basis recursively [PS 2011].

Newton bases allow to:

Properties

- Select the reconstruction lines;
- Solve a smaller system;
- Thanks to the selection of line-points we have a good compression of data.

How many Newton Bases ?

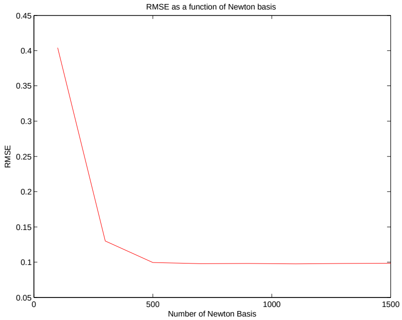

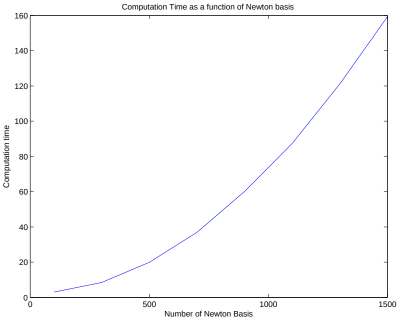

Number of (Newton bases) selected lines and computation time for Bull’s Eye phantom reconstruction

Selection Point

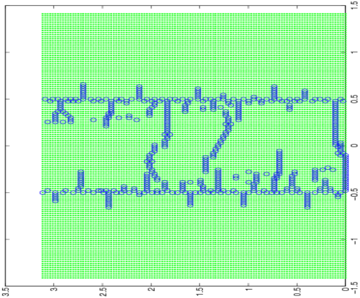

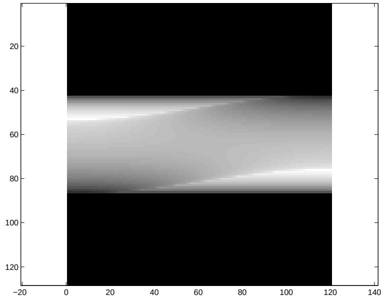

500 points are selected for the reconstruction of the Crescent Shape phantom sinogram instead of 1500

Line selection

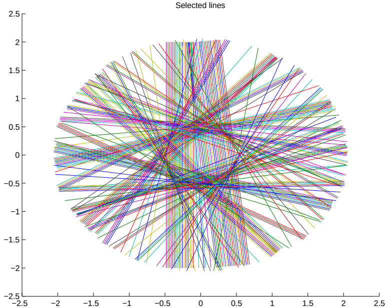

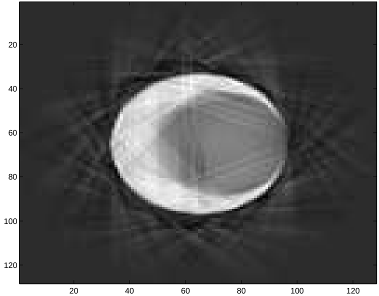

200 lines selected for the reconstruction of the Crescent Shape phantom: the phantom reconstructed with 200 Newton bases.

Double-weighted kernel methods vs ART methods

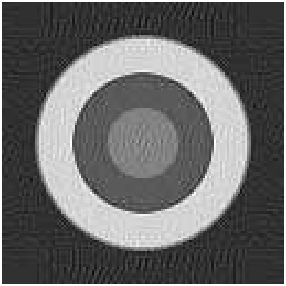

Figure: We compare a reconstruction with ART (first image) and the reconstruction with double-weighted kernel methods with 1500 (full data) Newton Bases (second image)

Double-weighted kernel methods vs ART methods

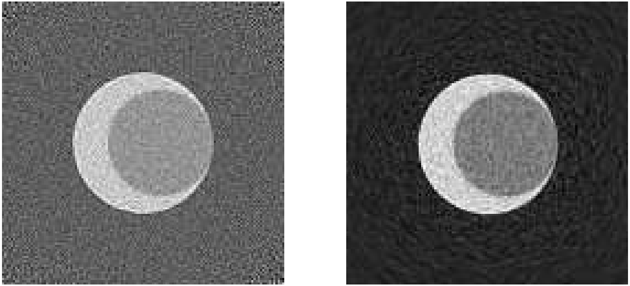

Figure: **Data with noise**: we compare a reconstruction with ART (first image) and the reconstruction with double-weighted kernel methods with 1500 Newton Bases (second image)

Double-weighted kernel methods vs ART methods

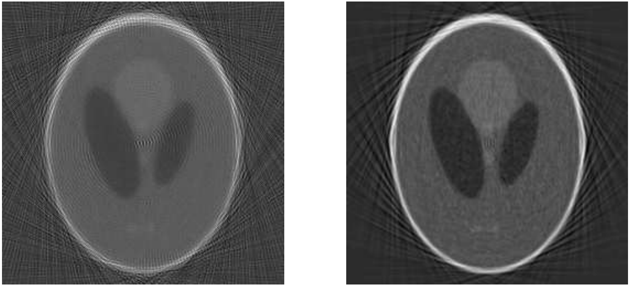

Figure: **Missing Data**: we compare a reconstruction with ART and the reconstruction with double-weighted kernel methods with 1500 Newton Bases (second image); Missing data: 40 % of Radon data

Summary and future work

Done

1. Filtered Back-Projection Formula
   - Efficiency
2. Kernel based reconstruction
   - Flexibility: double window function
   - Arbitrary scattered Radon data

To be done

1. More on the error analysis
2. Conditionally positive definite kernels
3. Efficiency

Thank you for your attention!